GANIT

GANIT: Journal of Bangladesh Mathematical Society

GANITJ. Bangladesh Math. Soc. 46.3 (2026) 082–090
DOI: https://doi.org/10.3329/ganit.v46i01.90168

Numerical Simulation of a Macroscopic Multilane Traffic Flow Model Based on Linear Velocity-Density Function

Md Rasel Ahmed [1], Jannatul Ferdous [2] Bitu Joydhar [3], Laek Sazzad Andallah [4], Prokriti Biswas [5]

[1]Department of Mathematics, Uttara University, Dhaka, Bangladesh, [2]Department of General Education, Netrokona University, Netrokona, Bangladesh, [3]Department of Mathematical & Physical Science, East West University, Dhaka ,Bangladesh, [4,5]Department of Mathematics, Jahangirnagar University, Dhaka, Bangladesh

ABSTRACT

Our present world is based on communication. Transportation is a major component of communication. For overpopulated countries in the world, a large number of vehicles are required for transportation, which causes traffic congestion. Traffic congestion is a critical issue in urban areas worldwide, particularly on multilane roadways where the complexity of interactions between vehicles can lead to significant delays, accidents, and reduced efficiency. Multilane traffic flow models have emerged as powerful tools to simulate and analyze traffic dynamics under various conditions.

In this paper, we assume a macroscopic multilane traffic flow model based on a linear velocity-density relationship, which yields a non-linear first-order system of hyperbolic partial differential (PDE) equations as an initial boundary value problem (IBVP). Since the analytical solution of the macroscopic multilane traffic flow model for two lanes is very complicated, there is a demand for efficient numerical methods to solve the macroscopic multilane traffic flow model. Due to the complexity of the analytical solution, we explore numerical solutions using the finite difference method, specifically the first-order Explicit Upwind Scheme, the Lax-Friedrich Scheme, and the second-order Lax-Wendroff Scheme. We determine the well-posedness and the stability analysis, and finally compare the three numerical schemes. The goal of this research is to contribute to the development of more efficient traffic management systems by providing insights into the movement and interaction of vehicles on multilane roads.

Received: November 09, 2025 **Accepted:** April 27, 2026, **Published Online:** June 15, 2026
Keywords: Macroscopic Multilane Traffic Flow Model, Explicit Upwind Scheme, Lax-Friedrich Scheme, Lax-Wendroff Scheme, Numerical Solution.

*Corresponding author: Email Address: raselju47@gmail.com, jannat@neu.ac.bd, bitujoydhar@gmail.com, andallah@juniv.edu, prokritimath42@juniv.edu

1. Introduction

In a microscopic framework, multilane traffic systems are typically described through individual vehicle interactions, where lane-changing (lane-sharing) events occur at the level of each vehicle. However, in a macroscopic framework, it is not feasible to track individual vehicles. Instead, traffic flow is treated as a continuous medium, analogous to fluid flow, where the primary variable is traffic density. In this continuum representation, the physical interpretation of a multilane system is based on an aggregate description of traffic rather than individual vehicle motion.

In particular, a two-lane system is modeled by considering each lane as a separate continuous density field. Lane-changing behavior is then interpreted as a transfer of traffic density between adjacent lanes rather than discrete vehicle movements. This interaction is incorporated through appropriate source and sink terms, which represent the average rate of exchange of vehicles between lanes. As a result, the evolution of traffic density in each lane is governed not only by its own flow dynamics but also by its coupling with the neighboring lane.

2. Mathematical Framework for the Macroscopic Multilane Traffic Flow Model

We assume a macroscopic multilane traffic flow model for two lanes, which is the following form

$$\left.\begin{aligned}\frac{\partial \rho_1}{\partial t}+\frac{\partial q_1(\rho)}{\partial x}&=\frac{\rho_2}{T_2^1}-\frac{\rho_1}{T_1^2}\\ \frac{\partial \rho_2}{\partial t}+\frac{\partial q_2(\rho)}{\partial x}&=\frac{\rho_1}{T_1^2}-\frac{\rho_2}{T_2^1}\end{aligned}\right\} \quad (1)$$

In this study, the two-lane macroscopic multilane traffic flow model (1) is formulated using the Greenshields linear velocity–density relationship. The linear velocity density relationship is

$$u(\rho)=u_{max}\left(1-\frac{\rho}{\rho_{max}}\right)$$

Where $u(\rho)$ represents the mean velocity at density ρ, ρ_{max} represents the maximum density or jam density, u_{max} represents the maximum velocity.

And the linear velocity-density relationship, the traffic flux is

$$q(\rho)=\rho u(\rho)=u_{max}\left(\rho-\frac{\rho^2}{\rho_{max}}\right)$$

3. Numerical Analysis of the Macroscopic Multilane Traffic Flow Model

Due to the complexity of the analytical solution, we focus on numerical approximations using finite difference methods, specifically the first-order Explicit Upwind scheme, the Lax-Friedrichs scheme, and the second-order Lax–Wendroff scheme. In this study, the governing PDE (1) is solved numerically within the finite difference method [3-5], [9-13]. The proposed macroscopic multilane traffic flow model is formulated under a linear velocity–density relationship and treated as an initial boundary value problem (IBVP) with prescribed left and right boundary conditions,

$$\frac{\partial \rho_1}{\partial t}+\frac{\partial q_1}{\partial x}=\frac{\rho_2}{T_2^1}-\frac{\rho_1}{T_1^2};\ a\le x\le b;\ t_o\le t\le T, T\ge 0 \quad (3.1)$$

$$\frac{\partial \rho_2}{\partial t}+\frac{\partial q_2}{\partial x}=\frac{\rho_1}{T_1^2}-\frac{\rho_2}{T_2^1};\ a\le x\le b;\ t_o\le t\le T, T\ge 0 \quad (3.2)$$

With the initial condition: $\rho_1(t_0,x)=(\rho_1)_0(x);\ a\le x\le b$

$\rho_2(t_0,x)=(\rho_2)_0(x);\ a\le x\le b$

And boundary condition: $\rho_1(t,a)=(\rho_1)_a(t);\ t_o\le t\le T$

$\rho_2(t,a)=(\rho_2)_a(t);\ t_o\le t\le T$

$\rho_1(t,b)=(\rho_1)_b(t);\ t_o\le t\le T$

$\rho_2(t,b)=(\rho_2)_b(t);\ t_o\le t\le T$

In this work, the numerical solution is evaluated using three schemes: the first-order Explicit Upwind scheme, the Lax-Friedrichs scheme, and the second-order Lax-Wendroff scheme.

4. Explicit Upwind Scheme

To build an Explicit Upwind Scheme, we discretize the time derivative $\frac{\partial \rho_1}{\partial t}$ and $\frac{\partial \rho_2}{\partial t}$ by first order forward difference formula, and we discretize the spatial derivative $\frac{\partial q_1}{\partial x}$ and $\frac{\partial q_2}{\partial x}$ by the first-order backward difference formula at any point (t^n, x_j), we get

$$\frac{\partial \rho_1}{\partial t}(t^n,x_j)\approx\frac{{\rho_1}_j^{n+1}-{\rho_1}_j^{n}}{\Delta t} \quad \text{and} \quad \frac{\partial \rho_2}{\partial t}(t^n,x_j)\approx\frac{{\rho_2}_j^{n+1}-{\rho_2}_j^{n}}{\Delta t} \quad (4.1)$$

$$\frac{\partial q_1}{\partial x}(t^n,x_j)\approx\frac{{q_1}_j^{n}-{q_1}_{j-1}^{n}}{\Delta x} \quad \text{and} \quad \frac{\partial q_2}{\partial x}(t^n,x_j)\approx\frac{{q_2}_j^{n}-{q_2}_{j-1}^{n}}{\Delta x} \quad (4.2)$$

Using equations (4.1) and (4.2) in equations (3.1) and (3.2), we get

$${\rho_1}_j^{n+1}={\rho_1}_j^{n}-\frac{\Delta t}{\Delta x}\left({q_1}_j^{n}-{q_1}_{j-1}^{n}\right)+\Delta t\left(\frac{{\rho_2}_j^{n}}{T_2^1}-\frac{{\rho_1}_j^{n}}{T_1^2}\right) \quad (4.3)$$

$${\rho_2}_j^{n+1}={\rho_2}_j^{n}-\frac{\Delta t}{\Delta x}\left({q_2}_j^{n}-{q_2}_{j-1}^{n}\right)+\Delta t\left(\frac{{\rho_1}_j^{n}}{T_1^2}-\frac{{\rho_2}_j^{n}}{T_2^1}\right) \quad (4.4)$$

For the linear velocity-density relationship, we have

$${q_1}_j^{n}=q\left({\rho_1}_j^{n}\right)={u_1}_{max}\left({\rho_1}_j^{n}-\frac{({\rho_1}_j^{n})^2}{{\rho_1}_{max}}\right) \quad (4.5)$$

$${q_2}_j^{n}=q\left({\rho_2}_j^{n}\right)={u_2}_{max}\left({\rho_2}_j^{n}-\frac{\left({\rho_2}_j^{n}\right)^2}{{\rho_2}_{max}}\right) \quad (4.6)$$

$$q_{1_{j-1}}^{\,n} = q\left(\rho_{1_{j-1}}^{\,n}\right) = u_{1_{max}}\left(\rho_{1_{j-1}}^{\,n} - \frac{\left(\rho_{1_{j-1}}^{\,n}\right)^2}{\rho_{1_{max}}}\right) \tag{4.7}$$

$$q_{2_{j-1}}^{\,n} = q\left(\rho_{2_{j-1}}^{\,n}\right) = u_{2_{max}}\left(\rho_{2_{j-1}}^{\,n} - \frac{\left(\rho_{2_{j-1}}^{\,n}\right)^2}{\rho_{2_{max}}}\right) \tag{4.8}$$

By using equations (4.5) and (4.7) in equation (4.3), we get,

$$\rho_{1_j}^{\,n+1} = \rho_{1_j}^{\,n} - \gamma_1\left(\left(\rho_{1_j}^{\,n} - \frac{\left(\rho_{1_j}^{\,n}\right)^2}{\rho_{1_{max}}}\right) - \left(\rho_{1_{j-1}}^{\,n} - \frac{\left(\rho_{1_{j-1}}^{\,n}\right)^2}{\rho_{1_{max}}}\right)\right) + \Delta t\left(\frac{\rho_{2_j}^{\,n}}{T_2^1} - \frac{\rho_{1_j}^{\,n}}{T_1^2}\right) \tag{4.9}$$

By using equations (4.6) and (4.8) in equation (4.4), we get

$$\rho_{2_j}^{\,n+1} = \rho_{2_j}^{\,n} - \gamma_2\left(\left(\rho_{2_j}^{\,n} - \frac{\left(\rho_{2_j}^{\,n}\right)^2}{\rho_{2_{max}}}\right) - \left(\rho_{2_{j-1}}^{\,n} - \frac{\left(\rho_{2_{j-1}}^{\,n}\right)^2}{\rho_{2_{max}}}\right)\right) + \Delta t\left(\frac{\rho_{1_j}^{\,n}}{T_1^2} - \frac{\rho_{2_j}^{\,n}}{T_2^1}\right) \tag{4.10}$$

Where, $\gamma_1 = u_{1_{max}}\left(\frac{\Delta t}{\Delta x}\right)$ and $\gamma_2 = u_{2_{max}}\left(\frac{\Delta t}{\Delta x}\right)$

Equations (4.9) and (4.10) correspond to the Explicit Upwind finite difference schemes for the two-lane traffic flow model based on a linear velocity–density relationship.

5. Lax-Friedrich Scheme

To build the Lax-Friedrich Scheme, we discretize the time derivative $\frac{\partial \rho_1}{\partial t}$ and $\frac{\partial \rho_2}{\partial t}$ by first order forward difference formula, and we discretize the spatial derivative $\frac{\partial q_1}{\partial x}$ and $\frac{\partial q_2}{\partial x}$ by the first-order central difference formula at any point (t^n, x_j), we obtain

$$\frac{\partial \rho_1}{\partial t}(t^n, x_j) \approx \frac{\rho_{1_j}^{\,n+1} - \rho_{1_j}^{\,n}}{\Delta t} \quad \text{and} \quad \frac{\partial \rho_2}{\partial t}(t^n, x_j) \approx \frac{\rho_{2_j}^{\,n+1} - \rho_{2_j}^{\,n}}{\Delta t} \tag{5.1}$$

$$\frac{\partial q_1}{\partial x}(t^n, x_j) \approx \frac{q_{1_{j+1}}^{\,n} - q_{1_{j-1}}^{\,n}}{2\Delta x} \quad \text{and} \quad \frac{\partial q_2}{\partial x}(t^n, x_j) \approx \frac{q_{2_{j+1}}^{\,n} - q_{2_{j-1}}^{\,n}}{2\Delta x} \tag{5.2}$$

By using equations (5.1) and (5.2) in equations (3.1) and (3.2) without the source term, we get

$$\rho_{1_j}^{\,n+1} = \rho_{1_j}^{\,n} - \frac{\Delta t}{2\Delta x}\left(q_{1_{j+1}}^{\,n} - q_{1_{j-1}}^{\,n}\right) \tag{5.3}$$

$$\rho_{2_j}^{\,n+1} = \rho_{2_j}^{\,n} - \frac{\Delta t}{2\Delta x}\left(q_{2_{j+1}}^{\,n} - q_{2_{j-1}}^{\,n}\right) \tag{5.4}$$

Equations (5.3) and (5.4) indicate the forward time central space (FTCS) scheme. From Von Neumann stability analysis, it ensures that the scheme is unconditionally unstable. But the scheme may be stable for sufficiently small $\frac{\Delta t}{\Delta x}$ and let us consider a modification of the FTCS scheme in which the term $\rho_{1_j}^{\,n}$ has been replaced by $\frac{1}{2}(\rho_{1_{j+1}}^{\,n} + \rho_{1_{j-1}}^{\,n})$. Then the FTCS scheme (5.3) becomes

$$\rho_{1_j}^{\,n+1} = \frac{1}{2}\left(\rho_{1_{j+1}}^{\,n} + \rho_{1_{j-1}}^{\,n}\right) - \frac{\Delta t}{2\Delta x}\left(q_{1_{j+1}}^{\,n} - q_{1_{j-1}}^{\,n}\right) \tag{5.5}$$

Now, adding the source term of (3.1) into (5.5), we get

$$\rho_{1_j}^{\,n+1} = \frac{1}{2}\left(\rho_{1_{j+1}}^{\,n} + \rho_{1_{j-1}}^{\,n}\right) - \frac{\Delta t}{2\Delta x}\left(q_{1_{j+1}}^{\,n} - q_{1_{j-1}}^{\,n}\right) + \Delta t\left(\frac{\rho_{2_j}^{\,n}}{T_2^1} - \frac{\rho_{1_j}^{\,n}}{T_1^2}\right) \tag{5.6}$$

Similarly, for the equation (3.2), we can write,

$$\rho_{2_j}^{\,n+1} = \frac{1}{2}\left(\rho_{2_{j+1}}^{\,n} + \rho_{2_{j-1}}^{\,n}\right) - \frac{\Delta t}{2\Delta x}\left(q_{2_{j+1}}^{\,n} - q_{2_{j-1}}^{\,n}\right) + \Delta t\left(\frac{\rho_{1_j}^{\,n}}{T_1^2} - \frac{\rho_{2_j}^{\,n}}{T_2^1}\right) \tag{5.7}$$

For the linear velocity-density relationship, we can write

$$q_{1_{j+1}}^{\,n} = q\left(\rho_{1_{j+1}}^{\,n}\right) = u_{1_{max}}\left(\rho_{1_{j+1}}^{\,n} - \frac{\left(\rho_{1_{j+1}}^{\,n}\right)^2}{\rho_{1_{max}}}\right) \tag{5.8}$$

$$q_{2_{j+1}}^{\,n} = q\left(\rho_{2_{j+1}}^{\,n}\right) = u_{2_{max}}\left(\rho_{2_{j+1}}^{\,n} - \frac{\left(\rho_{2_{j+1}}^{\,n}\right)^2}{\rho_{2_{max}}}\right) \tag{5.9}$$

$$q_{1_{j-1}}^{n} = q\left(\rho_{1_{j-1}}^{n}\right) = u_{1_{max}}\left(\rho_{1_{j-1}}^{n} - \frac{\left(\rho_{1_{j-1}}^{n}\right)^2}{\rho_{1_{max}}}\right) \tag{5.10}$$

$$q_{2_{j-1}}^{n} = q\left(\rho_{2_{j-1}}^{n}\right) = u_{2_{max}}\left(\rho_{2_{j-1}}^{n} - \frac{\left(\rho_{2_{j-1}}^{n}\right)^2}{\rho_{2_{max}}}\right) \tag{5.11}$$

Now, substituting (5.8) and (5.10) in equation (5.6), we get

$$\rho_{1_j}^{n+1} = \frac{1}{2}(\rho_{1_{j+1}}^{n} + \rho_{1_{j-1}}^{n}) - \frac{\gamma_1}{2}\left(\left(\rho_{1_{j+1}}^{n} - \frac{(\rho_{1_{j+1}}^{n})^2}{\rho_{1_{max}}}\right) - \left(\rho_{1_{j-1}}^{n} - \frac{(\rho_{1_{j-1}}^{n})^2}{\rho_{1_{max}}}\right)\right) + \Delta t\left(\frac{\rho_{2_j}^{n}}{T_2^1} - \frac{\rho_{1_j}^{n}}{T_1^2}\right) \tag{5.12}$$

Now, substituting (5.9) and (5.11) in equation (5.7), we get

$$\rho_{2_j}^{n+1} = \frac{1}{2}(\rho_{2_{j+1}}^{n} + \rho_{2_{j-1}}^{n}) - \frac{\gamma_2}{2}\left(\left(\rho_{2_{j+1}}^{n} - \frac{(\rho_{2_{j+1}}^{n})^2}{\rho_{2_{max}}}\right) - \left(\rho_{2_{j-1}}^{n} - \frac{(\rho_{2_{j-1}}^{n})^2}{\rho_{2_{max}}}\right)\right) + \Delta t\left(\frac{\rho_{1_j}^{n}}{T_1^2} - \frac{\rho_{2_j}^{n}}{T_2^1}\right)$$

Where, $\gamma_1 = u_{1_{max}}\left(\frac{\Delta t}{\Delta x}\right)$ and $\gamma_2 = u_{2_{max}}\left(\frac{\Delta t}{\Delta x}\right)$

Equations (5.12) and (5.13) correspond to the Lax-Friedrichs finite difference schemes for the two-lane traffic flow model based on a linear velocity–density relationship.

6. Lax-Wendroff Scheme

Formulation of the Lax-Wendroff Scheme for (3.1) and (3.2), we use the Lax-Friedrich scheme at $\left(t^n, x_{j+\frac{1}{2}}\right)$ and $\left(t^n, x_{j-\frac{1}{2}}\right)$ for half step size and the Leap-frog scheme at $\left(t^{n+\frac{1}{2}}, x_j\right)$ for half step size.

Step-(i): We take the Lax-Friedrichs scheme (5.6) for a half step at $\left(t^n, x_{j+\frac{1}{2}}\right)$ is

$$\rho_{1_{j+\frac{1}{2}}}^{n+\frac{1}{2}} = \frac{1}{2}\left(\rho_{1_{j+1}}^{n} + \rho_{1_j}^{n}\right) - \frac{\Delta t}{2\Delta x}\left(q_{1_{j+1}}^{n} - q_{1_j}^{n}\right) \tag{6.1}$$

And at $\left(t^n, x_{j-\frac{1}{2}}\right)$ is

$$\rho_{1_{j-\frac{1}{2}}}^{n+\frac{1}{2}} = \frac{1}{2}\left(\rho_{1_j}^{n} + \rho_{1_{j-1}}^{n}\right) - \frac{\Delta t}{2\Delta x}\left(q_{1_j}^{n} - q_{1_{j-1}}^{n}\right) \tag{6.2}$$

Step-(ii): (Leap-frog scheme)

To develop the Leap-frog scheme, we discretize both spatial and temporal derivatives using the central difference formula.

$$\frac{\partial \rho_1}{\partial t}(t^n, x_j) \approx \frac{\rho_{1_j}^{n+1} - \rho_{1_j}^{n-1}}{2\Delta t} \quad \text{and} \quad \frac{\partial q_1}{\partial x}(t^n, x_j) \approx \frac{q_{1_{j+1}}^{n} - q_{1_{j-1}}^{n}}{2\Delta x} \tag{6.3}$$

Using equation (6.3) in equations (3.1) without the source term, we obtain

$$\rho_{1_j}^{n+1} = \rho_{1_j}^{n-1} - \left(\frac{\Delta t}{\Delta x}\right)\left(q_{1_{j+1}}^{n} - q_{1_{j-1}}^{n}\right)$$

that is the required Leap-frog scheme.

We now implement the Leap-Frog scheme with a half-step discretization at $\left(t^{n+\frac{1}{2}}, x_j\right)$ is

$$\rho_{1_j}^{n+1} = \rho_{1_j}^{n} - \left(\frac{\Delta t}{\Delta x}\right)\left(q_{1_{j+\frac{1}{2}}}^{n+\frac{1}{2}} - q_{1_{j-\frac{1}{2}}}^{n+\frac{1}{2}}\right) \tag{6.4}$$

From the linear velocity-density relation, we have

$$q(\rho) = \rho u(\rho) = u_{max}\left(\rho - \frac{\rho^2}{\rho_{max}}\right) \text{ which implies}$$

$$q_{1_{j+\frac{1}{2}}}^{n+\frac{1}{2}} = q_1\left(\rho_{1_{j+\frac{1}{2}}}^{n+\frac{1}{2}}\right) = u_{1_{max}}\left(\rho_{1_{j+\frac{1}{2}}}^{n+\frac{1}{2}} - \frac{\left(\rho_{1_{j+\frac{1}{2}}}^{n+\frac{1}{2}}\right)^2}{\rho_{1_{max}}}\right) \tag{6.5}$$

$$q_{1_{j-\frac{1}{2}}}^{n+\frac{1}{2}} = q_1\left(\rho_{1_{j-\frac{1}{2}}}^{n+\frac{1}{2}}\right) = u_{1_{max}}\left(\rho_{1_{j-\frac{1}{2}}}^{n+\frac{1}{2}} - \frac{\left(\rho_{1_{j-\frac{1}{2}}}^{n+\frac{1}{2}}\right)^2}{\rho_{1_{max}}}\right) \tag{6.6}$$

Now, substituting equations (6.5) and (6.6) into equation (6.4), we get

$$\rho_{1_j}^{n+1} = \rho_{1_j}^{n} - u_{1_{max}}\left(\frac{\Delta t}{\Delta x}\right)\left(\left(\rho_{1_{j+\frac{1}{2}}}^{n+\frac{1}{2}} - \frac{\left(\rho_{1_{j+\frac{1}{2}}}^{n+\frac{1}{2}}\right)^2}{\rho_{1_{max}}}\right) - \left(\rho_{1_{j-\frac{1}{2}}}^{n+\frac{1}{2}} - \frac{\left(\rho_{1_{j-\frac{1}{2}}}^{n+\frac{1}{2}}\right)^2}{\rho_{1_{max}}}\right)\right) \tag{6.7}$$

Now, using equations (6.1) and (6.2) in equation (6.7), we get

$$\rho_{1_j}^{n+1} = \rho_{1_j}^{n} - \gamma_1\left(\frac{1}{2}\left(\rho_{1_{j+1}}^{n} - \rho_{1_{j-1}}^{n}\right) - \frac{\Delta t}{2\Delta x}\left(q_{1_{j+1}}^{n} - 2q_{1_j}^{n} + q_{1_{j-1}}^{n}\right)\right)\times$$
$$\left(1 - \frac{1}{\rho_{1_{max}}}\left(\frac{1}{2}\left(\rho_{1_{j+1}}^{n} + 2\rho_{1_j}^{n} + \rho_{1_{j-1}}^{n}\right) - \frac{\Delta t}{2\Delta x}\left(q_{1_{j+1}}^{n} - q_{1_{j-1}}^{n}\right)\right)\right) \tag{6.8}$$

Now, adding the source into the equation (6.8), we obtain

$$\rho_{1_j}^{n+1} = \rho_{1_j}^{n} - \gamma_1\left(\frac{1}{2}\left(\rho_{1_{j+1}}^{n} - \rho_{1_{j-1}}^{n}\right) - \frac{\Delta t}{2\Delta x}\left(q_{1_{j+1}}^{n} - 2q_{1_j}^{n} + q_{1_{j-1}}^{n}\right)\right)\times$$
$$\left(1 - \frac{1}{\rho_{1_{max}}}\left(\frac{1}{2}\left(\rho_{1_{j+1}}^{n} + 2\rho_{1_j}^{n} + \rho_{1_{j-1}}^{n}\right) - \frac{\Delta t}{2\Delta x}\left(q_{1_{j+1}}^{n} - q_{1_{j-1}}^{n}\right)\right)\right) + \Delta t\left(\frac{\rho_{2_j}^{n}}{T_2^1} - \frac{\rho_{1_j}^{n}}{T_1^2}\right) \tag{6.9}$$

Similarly, for equation (3.2), we get

$$\rho_{2_j}^{n+1} = \rho_{2_j}^{n} - \gamma_2\left(\frac{1}{2}\left(\rho_{2_{j+1}}^{n} - \rho_{2_{j-1}}^{n}\right) - \frac{\Delta t}{2\Delta x}\left(q_{2_{j+1}}^{n} - 2q_{2_j}^{n} + q_{2_{j-1}}^{n}\right)\right)\times$$
$$\left(1 - \frac{1}{\rho_{2_{max}}}\left(\frac{1}{2}\left(\rho_{2_{j+1}}^{n} + 2\rho_{2_j}^{n} + \rho_{2_{j-1}}^{n}\right) - \frac{\Delta t}{2\Delta x}\left(q_{2_{j+1}}^{n} - q_{2_{j-1}}^{n}\right)\right)\right) + \Delta t\left(\frac{\rho_{1_j}^{n}}{T_1^2} - \frac{\rho_{2_j}^{n}}{T_2^1}\right) \tag{6.10}$$

Where $q_{1_j}^{n} = q_1\left(\rho_{1_j}^{n}\right) = u_{1_{max}}\left(\rho_{1_j}^{n} - \frac{\left(\rho_{1_j}^{n}\right)^2}{\rho_{1_{max}}}\right)$

$$q_{2_j}^{n} = q_2\left(\rho_{2_j}^{n}\right) = u_{2_{max}}\left(\rho_{2_j}^{n} - \frac{\left(\rho_{2_j}^{n}\right)^2}{\rho_{2_{max}}}\right)$$

$$q_{1_{j\pm1}}^{n} = q_1\left(\rho_{1_{j\pm1}}^{n}\right) = u_{1_{max}}\left(\rho_{1_{j\pm1}}^{n} - \frac{\left(\rho_{1_{j\pm1}}^{n}\right)^2}{\rho_{1_{max}}}\right)$$

$$q_{2_{j\pm1}}^{n} = q_2\left(\rho_{2_{j\pm1}}^{n}\right) = u_{2_{max}}\left(\rho_{2_{j\pm1}}^{n} - \frac{\left(\rho_{2_{j\pm1}}^{n}\right)^2}{\rho_{2_{max}}}\right)$$

Equations (6.9) and (4.10) correspond to the Lax-Wendroff finite difference schemes for the two-lane traffic flow model based on a linear velocity–density relationship.

7. Well-Posedness and Stability Condition of Numerical Schemes

The implementation of the Explicit Upwind, Lax–Friedrichs, and Lax–Wendroff schemes is not straightforward because, in the considered traffic flow model, vehicles move in a single direction. As a result, the characteristic speed $q'\left(\rho_j^n\right)$must remain positive [1,2], [4], [6-8]. One needs to ensure the well-posedness condition

$$q'\left(c_j^n\right) \geq 0 \Rightarrow q'\left(c_j^n\right) = v_{max}\left(1 - \frac{2c_j^n}{c_{max}}\right) \geq 0 \quad \text{since } u_{max} > 0$$
$$\Rightarrow\ c_{max} \geq 2c_j^n \text{ which is the required well-posed condition}$$

By using a convex combination, we get the following stability condition

Table-1 : Stability Condition

Scheme	Formula	CFL/ Stability	Source-Term

Explicit Upwind	$\rho_j^{n+1} = (1-v)\rho_j^n + v\rho_{j-1}^n$	$0 \le v = \frac{u_{max}\Delta t}{\Delta x} \le 1$	$\Delta t \le \min(T_1^2, T_2^1)$
Lax-Friedrichs	$\rho_j^{n+1} = \left(\frac{1-v}{2}\right)\rho_{j-1}^n + \left(\frac{1+v}{2}\right)\rho_{j+1}^n$	$\lvert v\rvert = \left\lvert\frac{u_{max}\Delta t}{\Delta x}\right\rvert \le 1$	$\Delta t \le \min(T_1^2, T_2^1)$
Lax-Wendroff	$\rho_j^{n+1} = (1-v^2)\rho_j^n + \left(\frac{v}{2}\right)(1+v)\rho_{j-1}^n - \left(\frac{v}{2}\right)(1-v)\rho_{j+1}^n$	$\lvert v\rvert = \left\lvert\frac{u_{max}\Delta t}{\Delta x}\right\rvert \le 1$	$\Delta t \le \min(T_1^2, T_2^1)$

Where, $v = \frac{u_{max}\Delta t}{\Delta x}$ is the CFL number

8. Numerical Simulation and Result Discussion

To compute the density profile, the Explicit Upwind, Lax-Friedrichs, and Lax-Wendroff finite difference schemes are employed. For the numerical simulation of the macroscopic multilane traffic flow model with two lanes using these schemes, periodic initial and left boundary conditions are applied, while a Neumann boundary condition is imposed at the right boundary. The simulation is performed over a two-lane highway of 10 km length, representing the spatial domain [10], and the numerical experiment is conducted for a duration of 1.5 minutes. We assume 1800 spatial grid points with a spatial step size $\Delta x = 0.0056$ km and 405 temporal grid points with a step size $\Delta t = 0.2250$ seconds. We consider the maximum velocity of cars is $u_{1_{max}} = u_{2_{max}} = 60 km/hour = 0.0167 km/sec$ and maximum density ρ_{max} is evaluated by the following equations $\rho_{max} = k \times \max(\rho(0,x))$; $k \ge 2$. We choose k = 12; which implies $\rho_{1_{max}} = \rho_{2_{max}} = 660\ cars/km$ in the spatial domain [0, 10]. For the two-lane traffic flow model, we consider the car transition rate from lane 1 to lane 2 is 30% and from lane 2 to lane 1 is 40%

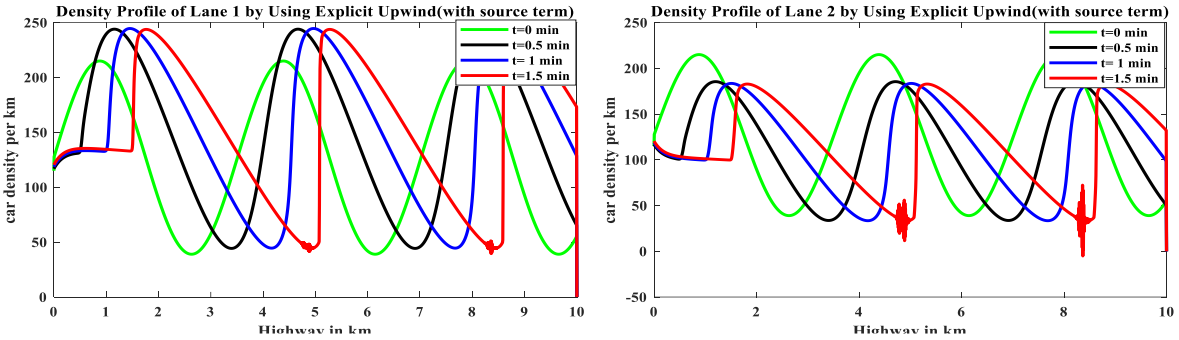

Figure-a: Development of numerical instability in the Explicit Upwind scheme due to violation of the stability criterion.

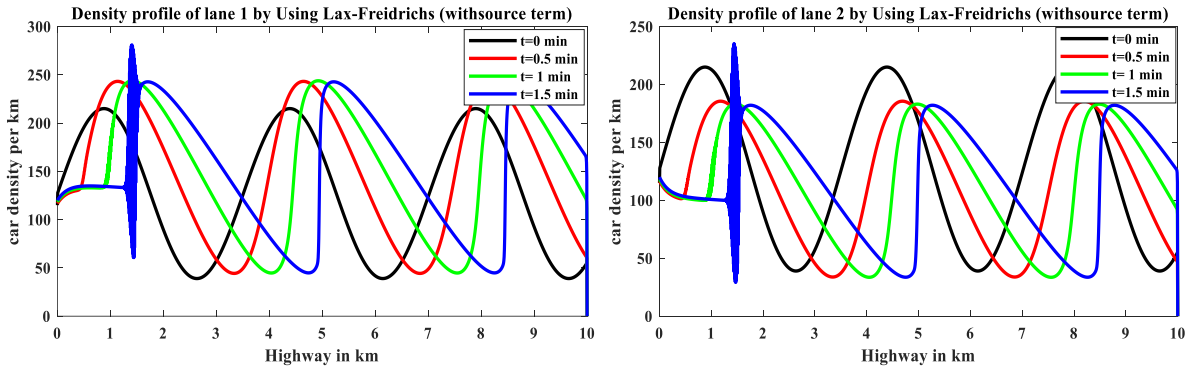

Figure-b: Development of numerical instability in the Lax-Friedrich scheme due to violation of the stability criterion.

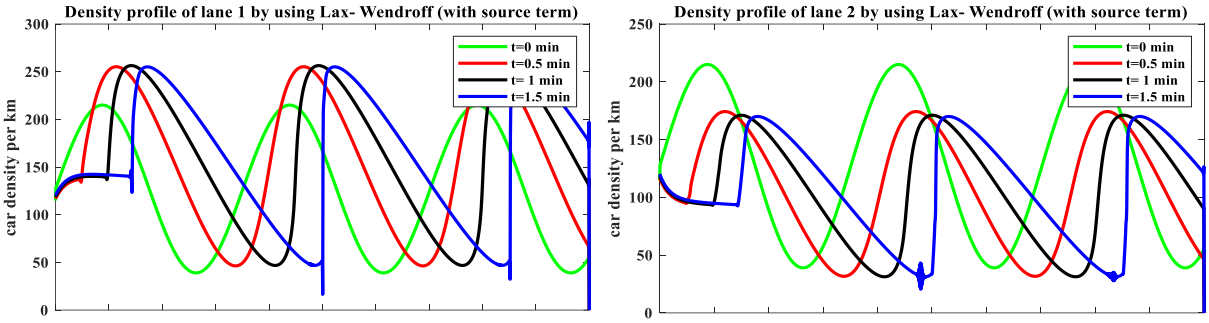

Figure-c: Development of numerical instability in the Lax-Wendroff scheme due to violation of the stability criterion.

These three figures a, b, c shows the unstable condition of Explicit Upwind Scheme, the Lax Friedrich Scheme, and the Lax-Wendroff scheme respectively. The reason of this instability is the violation of stability condition of table-1. Whereas the figures 1-6 indicate the stable condition of Explicit Upwind, Lax-Friedrich and Lax-Wendroff schemes, maintaining the stability condition of table-1.

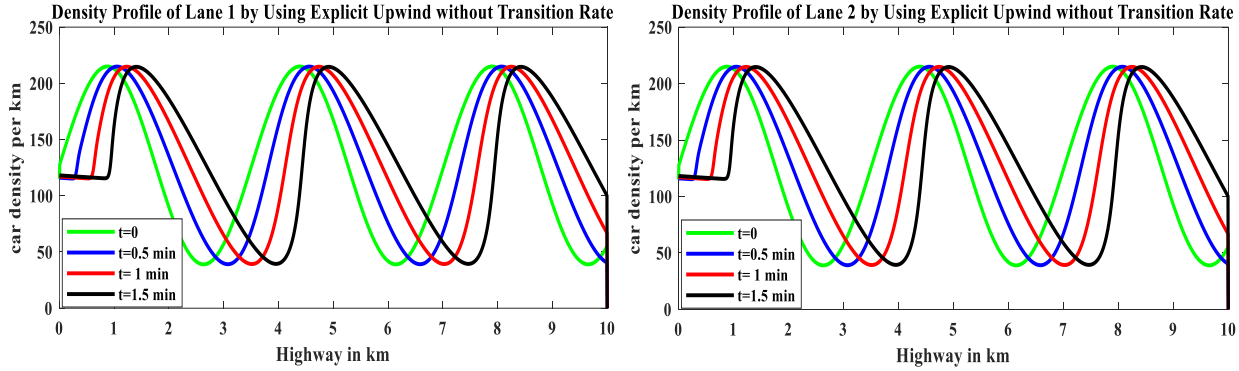

Figure 1: Density profile of Lane 1 and Lane 2 by using the Explicit Upwind Scheme without the transition rate

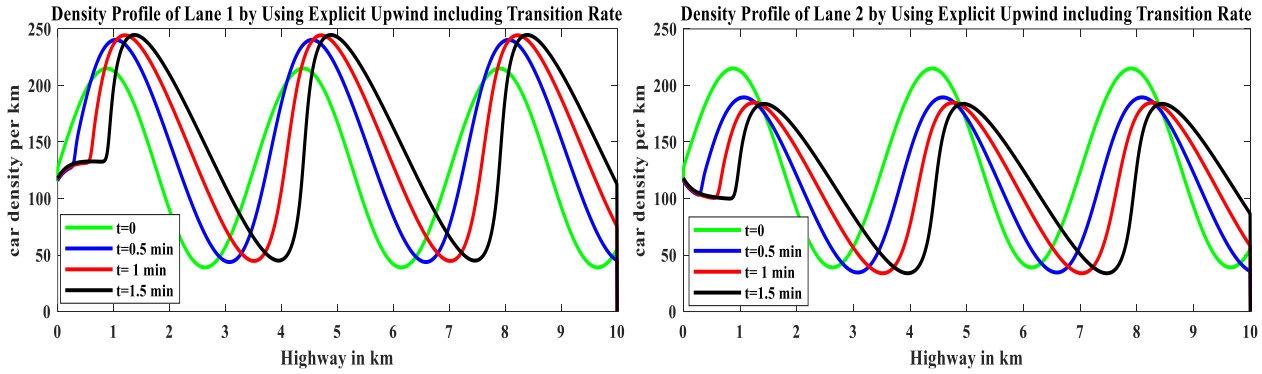

Figure 2: Density profile of Lane 1 and Lane 2 by using the Explicit Upwind Scheme, including the transition rate

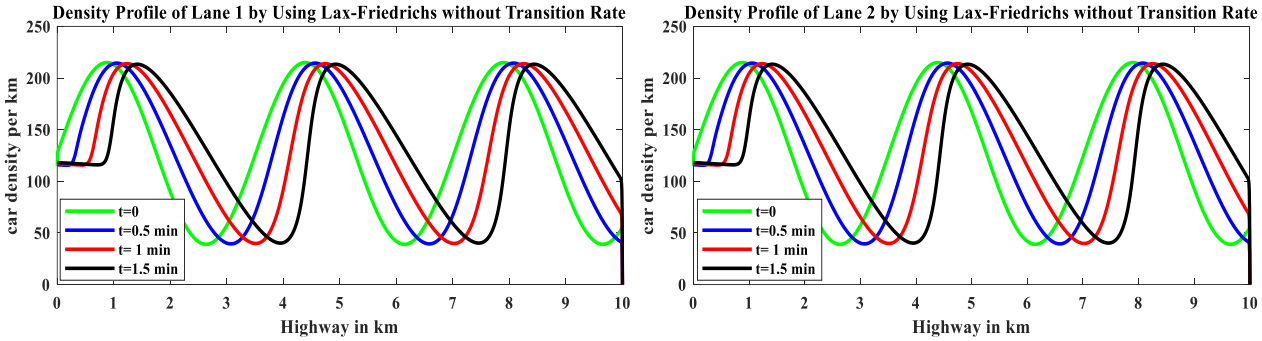

Figure 3: Density profile of Lane 1 and Lane 2 by using the Lax-Friedrichs Scheme without the transition rate

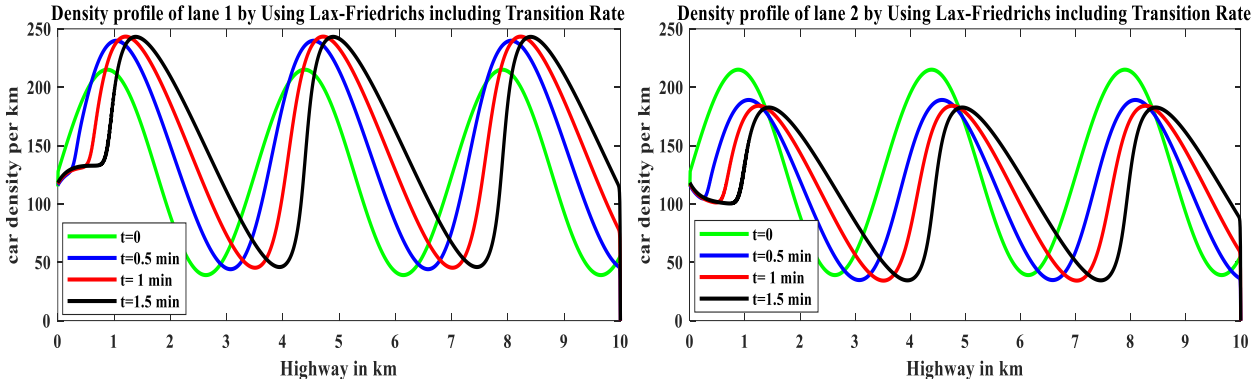

Figure 4: Density profile of Lane 1 and Lane 2 by using the Lax-Friedrichs Scheme, including the transition rate

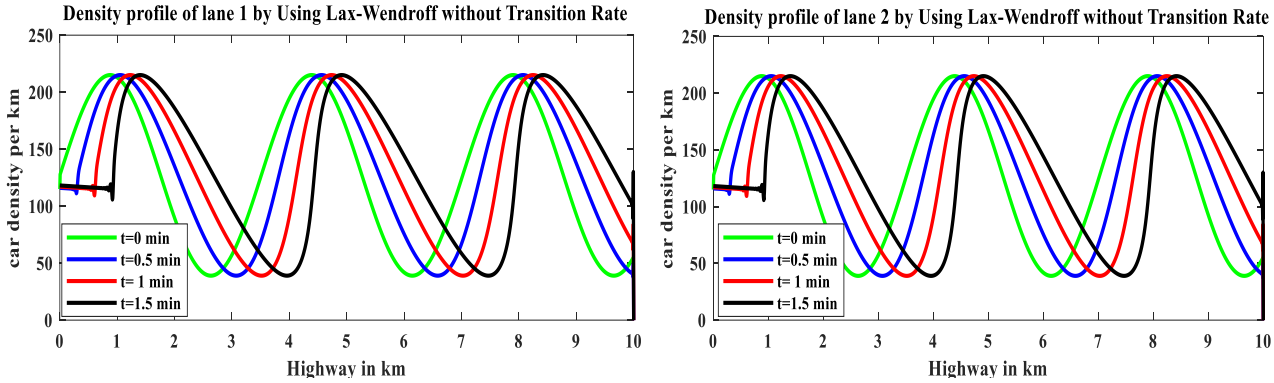

Figure 5: Density profile of Lane 1 and Lane 2 by using the Lax-Wendroff Scheme without the transition rate

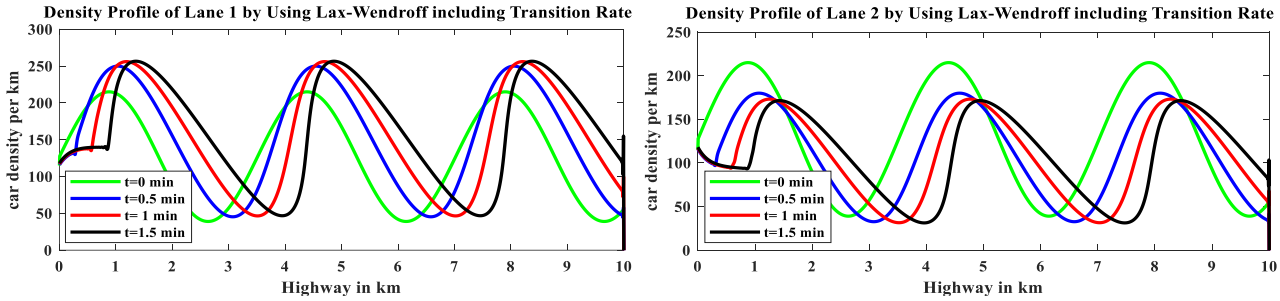

Figure 6: Density profile of Lane 1 and Lane 2 by using the Lax-Wendroff Scheme, including the transition rate

Figures 1–6 illustrate the numerical simulations of the density profiles for a two-lane macroscopic traffic flow model based on a linear velocity–density relationship. The simulations are conducted over a period of 1.5 minutes (90 seconds) using three finite difference schemes: the first-order Explicit Upwind Scheme, the Lax-Friedrichs Scheme, and the second-order Lax-Wendroff Scheme. The results depict the spatiotemporal evolution of vehicle density both without a transition rate and with the inclusion of a transition rate between lanes. When the transition rate is introduced, an increase in density is observed in lane 1, while a corresponding decrease occurs in lane 2. This behavior can be attributed to the greater density disparity between the two lanes, which induces a higher inter-lane vehicle transfer.

Table-2: Numerical Cost summary Table

Scheme	Order of accuracy	Relative CPU Time	Stability Limit (CFL)
Explicit Upwind	$O(\Delta x)$	1.528029 seconds	$\lvert v\rvert = \left\lvert \frac{u_{max}\Delta t}{\Delta x} \right\rvert \leq 1$
Lax-Friedrichs	$O(\Delta x)$	1.540715 seconds	$\lvert v\rvert = \left\lvert \frac{u_{max}\Delta t}{\Delta x} \right\rvert \leq 1$
Lax-Wendroff	$O(\Delta x^2)$	1.690567 seconds	$\lvert v\rvert = \left\lvert \frac{u_{max}\Delta t}{\Delta x} \right\rvert \leq 1$

9. Comparative Analysis of Explicit Upwind, Lax–Friedrich, and Lax– Wendroff Schemes

In this section, we evaluate the performance of the first-order Explicit Upwind scheme, the Lax-Friedrichs scheme, and the second-order Lax-Wendroff scheme in the context of the two-lane traffic flow model based on a linear velocity-density relation. A comparative analysis is conducted across various traffic flow parameters to evaluate their effectiveness. Based on the assumptions presented in Section 8, the numerical results for the density profiles, Figure 7 and Figure 8, are provided, facilitating a detailed comparison of the schemes' performance.

Table-3: Comparison Study Summary Table

Feature	Explicit Upwind/ Lax-Friedrichs	Lax-Wendroff
Numerical Dissipation	Leads to rounded peaks	Retains peak height
Gradient Profile	Smeared	steep
Wave Resolution	Lower details in shock transitions	High resolution of shocks

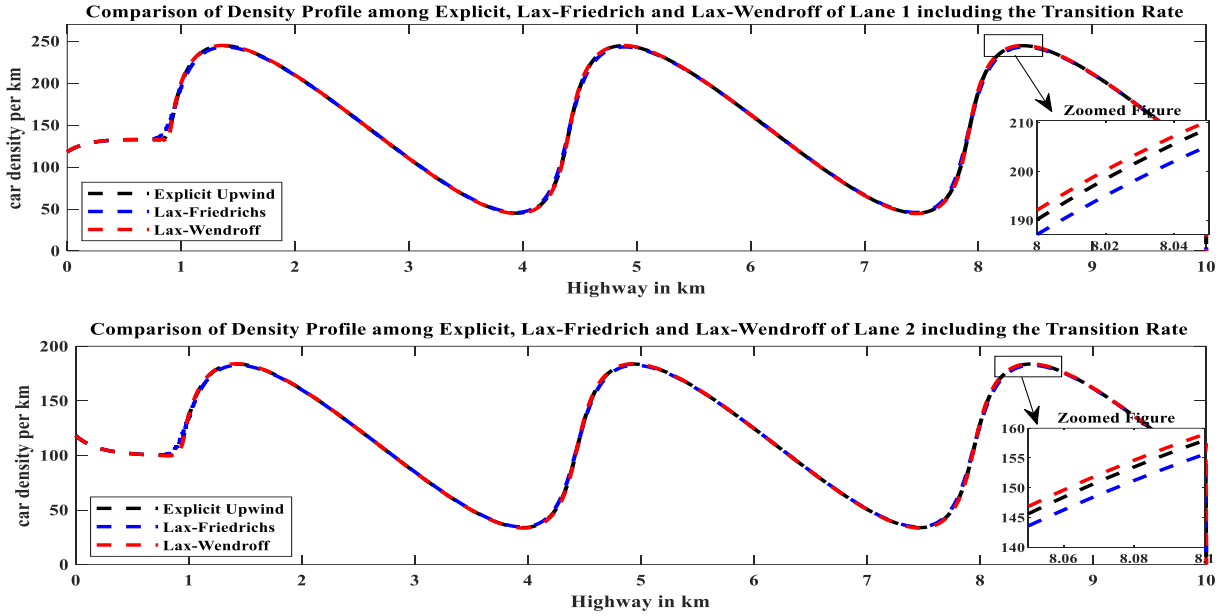

Figure 7: Density Profile Comparison for Explicit Upwind, Lax–Friedrich, and Lax–Wendroff Schemes

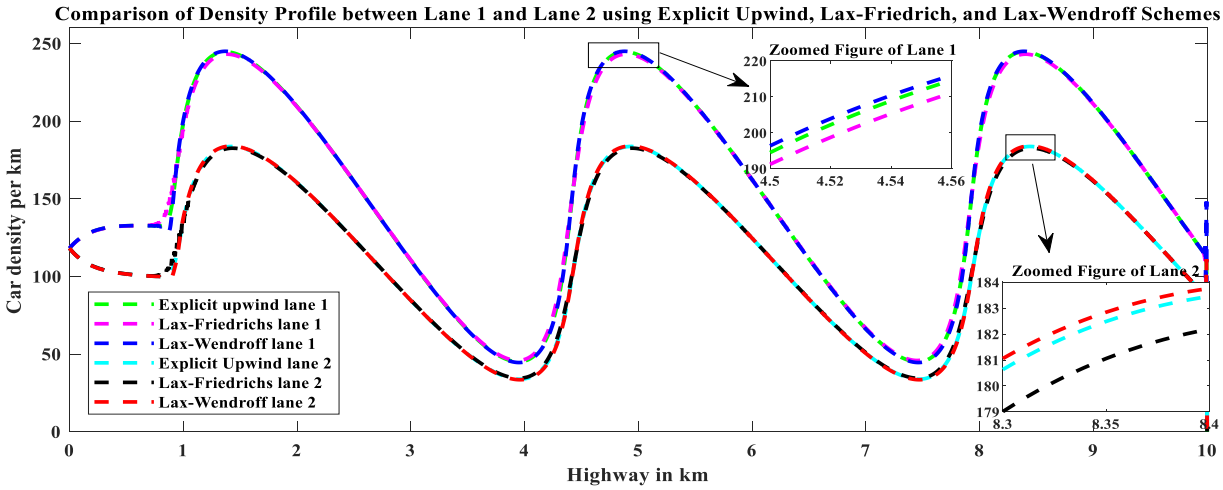

Figure 8: Comparison of Density Profile between Lane 1 and Lane 2 using Explicit Upwind, Lax-Friedrich, and Lax-Wendroff Schemes

The figures (7 & 8) present a comparative analysis of the car density profile for a two-lane traffic flow model using three numerical schemes: Explicit Upwind, Lax-Friedrichs, and Lax-Wendroff. In all cases, the global patterns of congestion waves, including the positions of density peaks and troughs, are consistent across the three methods, confirming the reliability of the schemes in capturing large-scale traffic dynamics. However, closer

inspection through the zoomed regions highlights important differences in accuracy. The Lax-Friedrich scheme exhibits the strongest numerical diffusion, resulting in lower peak densities compared to the other two schemes. This behavior reflects the inherent averaging property of the method, which smooths sharp gradients and reduces the fidelity of peak values. The Explicit Upwind scheme also introduces numerical diffusion; however, its results are closer to those of the Lax-Wendroff scheme, particularly in the main flow regions. The Lax-Wendroff scheme provides the most accurate resolution of steep gradients, preserving higher density peaks and sharper transitions without generating spurious oscillations under the chosen parameters. Furthermore, Lane 1 consistently shows higher density than Lane 2, indicating an unequal traffic load distribution. Overall, the analysis suggests that the Lax-Wendroff scheme offers the best balance of accuracy and stability for modeling multilane traffic flow.

10. Final Conclusion

This study compared the Explicit Upwind, Lax-Friedrichs, and Lax-Wendroff schemes for a macroscopic two-lane traffic flow model based on a linear velocity–density relation. The numerical results confirm that all schemes are stable and consistent, producing comparable density profiles for both lanes. Among them, the Lax–Wendroff scheme demonstrates higher accuracy and better resolution of sharp gradients, while the Explicit Upwind and Lax-Friedrichs schemes exhibit slightly greater numerical diffusion. When the lane transition rate is introduced, the spatiotemporal evolution of density effectively captures realistic inter-lane interactions and downstream wave propagation. Overall, the Lax-Wendroff method provides the most precise approximation of traffic behavior, whereas the other schemes offer satisfactory results with lower computational effort. These outcomes validate the reliability of the proposed framework and establish a foundation for extending the model to more complex multilane traffic systems.

Conflicts of Interest

The authors state that there are no conflicts of interest regarding the research, authorship, or publication of this article.

References

[1] Ahmed, M. R., Joydhar, B., Andallah, M. L. S., Biswas, P., & Ferdous, J. (2025). Numerical simulation of multilane traffic flow model based on exponential velocity–density function. Partial Differential Equations in Applied Mathematics, 16, 101323.
[2] Payne, H. J. (1979). A macroscopic simulation model of freeway traffic. Transportation Research Record, 722, 68–76.
[3] Kabir, M. H., & Andallah, L. S. (2013). Numerical simulation of multilane traffic flow model. GANIT: Journal of Bangladesh Mathematical Society, 33, 25–32.
[4] Helbing, D., & Greiner, A. (1997). Modelling and simulation of multilane traffic flow. Physical Review E, 55(5), 5498–5508.
[5] Colombo, R. M., & Rossi, E. (2006). Well-posedness for multilane traffic model. Annali dell'Università di Ferrara, 52, 291–301.
[6] Andallah, L. S., Ali, M. S., Akhter, J., Gani, M. O., & Pandit, M. K. (2008). A finite difference scheme of traffic flow model based on linear velocity–density function. Jahangirnagar University Journal of Science, 32(1), 57–67.
[7] Holden, H., & Risebro, N. H. (2019). Models for dense multilane vehicular traffic. SIAM Journal on Mathematical Analysis, 51(5), 3694–3713.
[8] Haque, M., Sultana, M., & Andallah, L. S. (2023). Numerical simulation of diffusion type traffic flow model using second-order Lax–Wendroff scheme based on exponential velocity density function. American Journal of Computational Mathematics, 13, 398–411.
[9] Klar, A., Kühne, R. D., & Wegener, R. (1999). A hierarchy of models for multilane vehicular traffic I: Modeling. SIAM Journal on Applied Mathematics, 59(3), 983–1001.
[10] Ali, M. S., & Andallah, L. S. (2019). Numerical solution of a multilane fluid dynamic traffic flow model with three lanes. IOSR Journal of Mathematics, 15(2), 1–10.
[11] Colombo, R. M., & Goatin, P. (2007). On multilane traffic flow. Communications in Mathematical Sciences, 1, 1–15.
[12] Hasan, M., Sultana, S., Andallah, L. S., & Azam, T. (2015). Lax–Friedrich scheme for the numerical simulation of a traffic flow model based on a nonlinear velocity density relation. American Journal of Computational Mathematics, 5, 186–194.
[13] Bretti, G., Natalini, R., & Piccoli, B. (2007). A fluid-dynamic traffic model on road networks. Barcelona, Spain: Computational Methods in Engineering.